MINERALOGICAL MAGAZINE

VOLUME 48 NUMBER 347 JUNE 1984

Mineral chemistry of regional chloritoid assemblages in the Chlorite Zone, Lycian Nappes, South-west Turkey

J. R. ASHWORTH

Department of Geological Sciences, University of Aston in Birmingham, Gosta Green, Birmingham B4 7ET

AND

M. M. EVIRGEN

Hidrojeoloji Mühendisliği Bölümü, Mühendislik Fakültesi, Hacettepe Üniversitesi, Beytepe Kampüsü, Ankara, Turkey

ABSTRACT. In the Ören area at the base of the Lycian Nappes, chloritoid is common on a regional scale. Mn and inferred Fe^{3+} contents are low. Chloritoid + quartz occur rather than the more hydrous equivalent pyrophyllite + chlorite, Fe/(Fe + Mg) values in chlorite ranging down to 0·27. Calcite and dolomite, which coexist with chloritoid and pyrophyllite, give a temperature estimate of 350 ± 30 °C, implying moderate to high activities of water for pyrophyllite stability. Muscovite–paragonite geothermometry is unreliable. Mg/Fe distribution coefficients between chloritoid and chlorite differ systematically from literature values from higher grades (biotite and garnet zones). Intensity of colour in chloritoid correlates with inferred Fe^{3+} content, which decreases outwards in grains showing prograde growth zoning.

IN many terrains, chloritoid is common at low grade (Winkler, 1979, p. 210), within what is traditionally known as the chlorite zone of the greenschist facies. Few compositional data have been published for chloritoid and coexisting minerals at lower grades than the garnet zone. These few studies concentrate on unusual assemblages with, for example, Fe–Mg carbonates (Cruickshank and Ghent, 1978) or Mn-rich silicates (Kramm, 1973). It is inferred that chloritoid can be stabilized by high Mn content (Kramm, 1973; Brindley and Elsdon, 1974). Very low activity of water, a_{H_2O}, is also inferred for some very low-grade occurrences (Frey, 1978) and some of the unusual assemblages (Cruickshank and Ghent, 1978). Low a_{H_2O} is consistent with the temperatures inferred in these studies (200–360 °C) being lower than those calculated at $a_{H_2O} = 1$ (Hoschek, 1969; Baltatzis, 1980) for the equilibrium

$$\text{pyrophyllite} + \text{chlorite} \rightleftharpoons \text{chloritoid} + \text{quartz} + H_2O. \quad (1)$$

Records of calcite and dolomite (Katagas and Sapountzis, 1977; Frey, 1978; Mposkos and Perdikatzis, 1981) also imply $a_{H_2O} < 1$. All attempts at geothermometry of low-grade chloritoid assemblages have been very indirect; calculations for equilibrium (1) are also suspect, because the thermochemical properties of chloritoid are poorly known (Helgeson *et al.*, 1978). In this paper, calcite–dolomite geothermometry is used to estimate the temperature of regional chloritoid development. Simple equilibria not involving chloritoid, are used to put limits on a_{H_2O} in the chloritoid-carbonate assemblages. Systematic relations between the composition of chloritoid and coexisting minerals are also investigated.

Geological setting. The area studied (fig. 1) is in the basal part of the Lycian Nappe complex. The nappes, formed from Permian to Cretaceous sedimentary rocks, are allochthonous relative to the

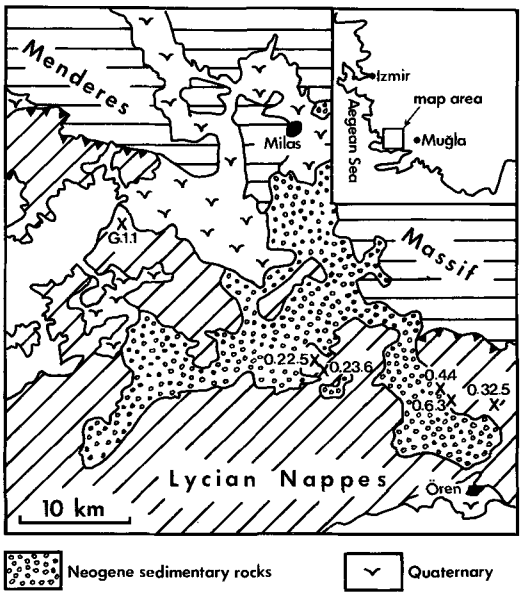

FIG. 1. Specimen location map. Geology simplified from the work of the MTA Institue (Çağlayan *et al.*, 1980).

underlying Menderes Massif and were probably emplaced in the Eocene (Gutnic *et al.*, 1979). The predominant lithologies near the base of the nappes are pelites (slates and phyllites) and slightly metamorphosed limestones. Pelites are commonest in the belt sampled, immediately above the basal tectonic discontinuity (fig. 1); limestones predominate at slightly higher structural level, further south.

Petrography. Chlorite assemblages predominate in pelites, though biotite occurs sporadically (perhaps reflecting low a_{H_2O}). Biotite is not found with chloritoid. Chloritoid is common, as scattered small laths which often form radiating clusters, in a wide range of lithologies, including highly aluminous pelites (fig. 2*a*), quartzose rocks of which fig. 2*b* shows a semipelitic variety, and calcareous assemblages which originated as impure limestones (fig. 2*c*). Table I gives the mineral assemblages in representative specimens selected for electron microprobe analysis. Pyrophyllite has not been found with chlorite.

Chloritoid usually shows distinctive pleochroism (α green or bluish green, β slaty blue or greenish blue, γ colourless or pale yellow), but in G.1.1 it is very pale yellow and almost non-pleochroic.

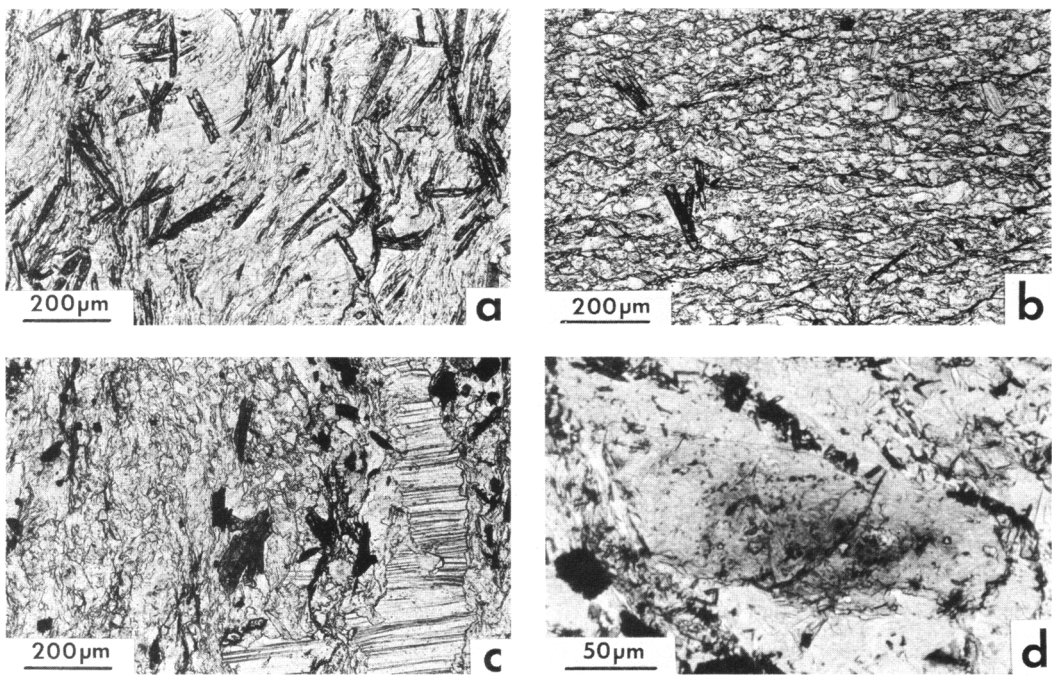

FIG. 2. Photomicrographs of chloritoid occurrences, in plane polarized light. (*a*) Abundant chloritoid with pyrophyllite and quartz, specimen O.4.4. (*b*) Chloritoid in quartzose phyllite with chlorite and muscovite, O.22.5. (*c*) Chloritoid with fine-grained muscovite and quartz, intimately associated with calcite (e.g. the large grain at the right) and hematite, O.6.3. (*d*) A zoned crystal of chloritoid, darker near its centre, with muscovite, chlorite, and rutile, O.32.5.

Intensity of colour varies within a specimen, and in O.32.5 there is obvious zoning (fig. 2*d*). In a few grains, this zoning has a rough hourglass shape.

Mineral compositions. The data for chloritoid and chlorite (Table II), and for paragonite and pyrophyllite (Table III) are representative point analyses by electron microprobe. Fe^{3+} in chloritoid is estimated by minimizing the sum of squares of deviations from the theoretical totals of the cation groups (respectively 2, 4, and 2). The zoning in O.32.5 is exemplified by analyses of the centre and edge of a single chloritoid grain (Table II). Analyses of muscovite coexisting with the paragonite and pyrophyllite of Table III are presented in a regional study of muscovites (Evirgen and Ashworth, 1983). The calcite and dolomite data (Table IV), for use in geothermometry, are averages of several point analyses (which show little variation). An analysis of coarse hematite is also presented in Table IV. Fine, disseminated opaque grains were confirmed to be hematite by semiquantitative microprobe work.

TABLE I. *Mineral assemblages in specimens used for microanalysis*

	G.1.1	O.4.4	O.6.3	O.22.5	O.23.6	O.32.5
Quartz	x	x	x	x	x	x
Muscovite		x	x	x	x	x
Chloritoid	x	x	x	x	x	x
Chlorite			x	x	x	x
Pyrophyllite	x	x				
Paragonite				x		
Calcite	x		x			
Dolomite	x					
Hematite		x	x		x	
Rutile	x	x		x	x	x

Interpretation

Partition of Fe *and* Mg *between chloritoid and chlorite.* The range of Fe/(Fe+Mg) ratios of chloritoid and chlorite is illustrated in the relevant part of the AFM diagram (fig. 3). All Fe is treated together at this stage; the Fe^{3+} content of chloritoid is discussed separately below. The chlorite data plotted are averages of several grains which show only slight variation within a specimen. The ranges of chloritoid composition in three specimens (O.6.3, O.22.5, and O.32.5) are shown diagrammatically

TABLE II. *Chloritoid and chlorite analyses*

	Chloritoid G.1.1	O.4.4	O.6.3	O.22.5	O.23.6	O.32.5 Centre	O.32.5 edge	Chlorite O.6.3	O.22.5	O.23.6	O.32.5
SiO_2	23.60	23.39	23.95	23.81	23.99	24.00	24.19	29.22	24.41	25.95	25.12
TiO_2	0.01	0.04	0.03	0.29	0.03	0.11	0.07	0.03	0.03	0.05	0.05
Al_2O_3	39.90	39.87	39.75	39.55	39.01	39.07	40.18	26.04	24.59	25.04	24.93
FeO*	26.82	25.79	25.11	25.58	26.48	25.86	22.95	12.25	24.66	21.83	18.69
MnO	0.12	0.17	0.59	0.25	0.26	0.32	0.43	0.08	0.07	0.09	0.06
MgO	1.15	1.81	3.04	2.05	2.35	2.46	3.46	19.43	14.20	15.40	18.25
CaO	0.03	0.00	0.00	0.00	0.00	0.02	0.02	0.06	0.00	0.03	0.03
H_2O†	7.09	7.07	7.20	7.12	7.13	7.13	7.20	12.31	11.48	11.77	11.75
Total	98.74	98.11	99.67	98.65	99.25	98.96	98.51	99.42	99.44	100.16	98.88
Recalculated to 12 oxygens (anhydrous)								Recalculated to 28 oxygens (anhydrous)			
Si	1.990	1.977	1.981	1.997	2.002	2.004	2.007	Si 5.690	5.094	5.281	5.123
								Al^{iv} 2.310	2.906	2.719	2.877
Al	3.966	3.972	3.876	3.911	3.837	3.847	3.930				
Ti	0.001	0.002	0.002	0.018	0.002	0.007	0.005	Al^{vi} 3.667	3.145	3.290	3.116
Fe^{3+}‡	0.040	0.046	0.136	0.069	0.157	0.139	0.057	Ti 0.004	0.005	0.008	0.007
Total	4.01	4.02	4.01	4.00	4.00	3.99	3.99	Fe 1.995	4.304	3.715	3.187
								Mn 0.012	0.012	0.015	0.011
Fe^{2+}	1.851	1.776	1.602	1.726	1.691	1.667	1.536	Mg 5.638	4.418	4.672	5.547
Mn	0.009	0.013	0.041	0.018	0.018	0.023	0.030	Ca 0.012	0.000	0.007	0.006
Mg	0.145	0.229	0.374	0.256	0.292	0.306	0.428				
Ca	0.003	0.000	0.000	0.000	0.000	0.002	0.001				
Total	2.01	2.02	2.02	2.00	2.00	2.00	2.00	Total 11.33	11.88	11.71	11.87

* Total Fe as FeO.
† H_2O calculated from formula with 4 (OH) in chloritoid, 16 (OH) in chlorite.
‡ Fe^{3+} in chloritoid estimated from stoichiometry.

by bars. Though individual point analyses scatter about the bars, they clearly define the trends shown. The variation in O.32.5 is simple zoning, correlated with the colour zoning; Fe/(Fe + Mg) decreases outwards. In chlorite coexisting with chloritoid, the lowest Fe/(Fe + Mg) value found is 0.27. Thus, in our area, chlorites at least as magnesian as this were involved in the chloritoid-producing reaction (1), which is a continuous reaction eliminating progressively more magnesian chlorite + pyrophyllite pairs with increasing grade (Zen, 1960).

The disparity between Fe/(Fe + Mg) in chloritoid and chlorite is greater in our area than in the garnet zone, so that the low-grade chloritoid + chlorite paragenesis represents rock compositions that would develop garnet at higher grade (dashed triangle in fig. 3). In treating the Fe, Mg distribution, the variation in chloritoid composition within a rock should be taken into account. The zoning in O.32.5 is in the direction expected from prograde operation of reaction (1), and is thus interpreted as prograde growth zoning, centres of grains retaining early formed compositions: at this low grade, small chloritoid grains evidently behave as refractory in the sense of Hollister (1969). Extending this interpretation to the irregular variation in chloritoid in other rocks, minimum Fe/Mg values for this mineral are used with chlorite averages from our specimens, for comparison with other areas (fig. 4). Because of the indeterminacy of Fe^{3+} in electron microprobe analyses, total Fe is used; this probably introduces negligible error, because there are usually indications that Fe^{3+} is low in chloritoid (cf. next section). The distribution coefficient calculated here is

$$K_D \begin{matrix} \text{Fe/Mg} \\ \text{chloritoid/chlorite} \end{matrix} = \frac{(\text{Fe/Mg})_{\text{chloritoid}}}{(\text{Fe/Mg})_{\text{chlorite}}}$$

The literature data are all from areas in which higher grade is indicated by the systematic occurrence (with chloritoid or nearby) of one or more of the following: biotite, garnet, staurolite, andalusite, and kyanite. These data clearly define a lower range of K_D than we observe: only two literature studies overlap our range, one (Liou and Chen, 1978) in an area of possibly similar grade (biotite being scarce), the other represented by an outlying, clearly anomalous point from the data-set of Rumble (1978). We infer that $K_{D\text{chloritoid/chlorite}}^{\text{Fe/Mg}}$, like other distribution coefficients (Thompson, 1976) tends towards unity with increasing temperature of equilibration. This distribution cofficient could prove useful as a grade indicator in low-grade rocks, extending below the range of common occurrence of biotite (which is used in most Fe, Mg distribution studies in pelites: Thompson, 1976). It could be

TABLE III. *Paragonite and pyrophyllite analyses*

	Paragonite O.22.5	Pyrophyllite O.4.4
SiO_2	47.48	66.47
TiO_2	0.09	0.02
Al_2O_3	39.50	28.19
FeO*	0.65	0.42
MnO	0.00	0.00
MgO	0.27	0.02
CaO	0.08	0.02
Na_2O	7.57	0.10
K_2O	0.55	0.11
H_2O†	4.73	4.99
Total	100.90	100.35
Recalculated to 22 oxygens (anhydrous)		
Si	6.015	7.974
Al^{iv}	1.985	0.026
Al^{vi}	3.915	3.961
Ti	0.008	0.002
Fe	0.069	0.042
Mn	0.000	0.000
Mg	0.051	0.004
Total	4.04	4.01
Ca	0.010	0.003
Na	1.858	0.023
K	0.088	0.017
Total	1.96	0.04

* Total Fe as FeO.
† H_2O calculated from formula with 4 (OH).

TABLE IV. *Calcite, dolomite and hematite analyses*

	Calcite G.1.1	Dolomite G.1.1		Hematite O.6.3
FeO*	1.66	15.54	TiO_2	1.39
MnO	0.22	0.48	Al_2O_3	0.06
MgO	0.45	10.02	Fe_2O_3*	97.95
CaO	53.25	29.55	MnO	0.02
CO_2†	43.44	43.94	MgO	0.00
Total	99.02	99.52	Total	99.42
Fe	0.047	0.435	Al	0.004
Mn	0.007	0.013	Ti	0.056
Mg	0.023	0.498	Mg	0.000
Ca	1.925	1.056	Fe	3.921
			Mn	0.001
Total	2.00	2.00	Total	3.98

* Total Fe as FeO in carbonates, Fe_2O_3 in hematite.
† CO_2 estimated from formula for carbonates.

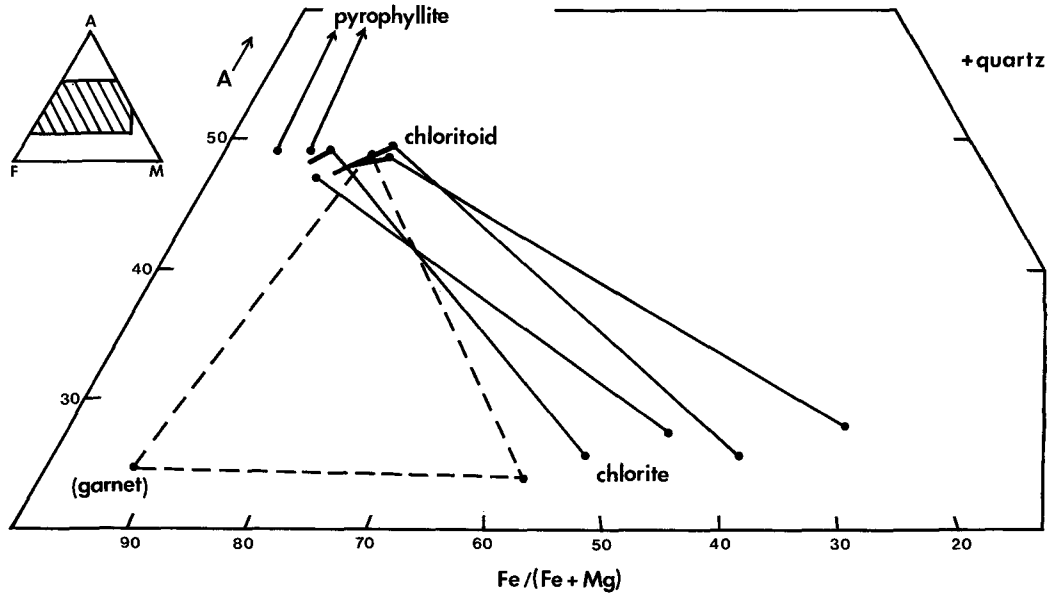

FIG. 3. AFM diagram of coexisting minerals, with total iron taken as FeO. Heavy bars represent zoning in chloritoid. Dashed lines indicate coexisting garnet, chloritoid, and chlorite found in the garnet zone of the Menderes Massif (Ashworth and Evirgen, 1983).

informative where other grade indicators are lacking or ambiguous, notably where the chloritoid assemblage has been produced by a retrograde event (e.g. Atherton, 1980).

Ferric iron content and colour of chloritoid. Chloritoid coexisting with pyrophyllite has high Al (Table II; fig. 3), implying low Fe^{3+}. The pyrophyllite, which has almost ideal composition (Table III), effectively saturates the Al content of the chloritoid (whether or not hematite is present). In chloritoid without pyrophyllite, the Fe/Mg variation noted above is correlated with a variation in Al content (fig. 3), indicating less substitution of Fe^{3+} for Al in the later-formed, higher-grade parts of a grain. This indicates a genuine decrease in the degree of oxidation of the rock during prograde metamorphism, as distinct from the reaction

$$\text{chlorite} + \text{hematite} \rightarrow \text{chloritoid} + \text{quartz} + \text{magnetite} + H_2O$$

(Thompson and Norton, 1968), which did not operate in the assemblages studied.

Differences in intensity of colour can be ascribed to different Fe^{3+} contents in the chloritoids studied. The pale colour of the particularly Fe-rich chloritoid in G.1.1. is unusual (Deer *et al.*, 1982), but this chloritoid has the lowest inferred content of *ferric* iron (Table II). The colour zoning in O.32.5 similarly correlates with inferred Fe^{3+}, and there is no other compositional variation (Table II) which could account for the striking colour change (fig. 2*d*). Thus the present work is highly consistent with the finding of Hålenius *et al.* (1981) that the colour of chloritoid becomes more intense with increasing $[Fe^{3+}][Fe^{2+}]$ concentration product, rather than simply Fe^{2+} content. Mössbauer determinations of Fe^{3+} by Hålenius *et al.* (1981) bring the cation group totals close to the ideal values, further justifying our method of recalculation. The substitution of Fe^{3+}, O^{2-} for Fe^{2+}, OH^- (Deer *et al.*, 1982, p. 872) thus appears to be uncommon, and need not be invoked in this study. This substitution would lead to lower than ideal H_2O contents: *higher* than ideal H_2O might be suggested on the basis of our low totals (Table II), but these can probably be explained simply by the ubiquitous cracks in the chloritoid.

Physical conditions of metamorphism. It is of interest to assess the conditions of formation of these widespread assemblages, in which chloritoid does not have unusual composition: Mn contents are low in all the minerals (including hematite, Table IV), and it is unlikely that the Fe^{3+} content of chloritoid is sufficient to be a major factor in its stability.

Temperature can be estimated, and constraints placed on a_{H_2O}, in the carbonate-bearing assemblages. The result depends slightly on total pressure. Calculations were carried out for $P = 3$ kbar, which is an educated guess following the study of

muscovite compositions (Evirgen and Ashworth, 1983). An uncertainty of ± 1 kbar has negligible effect on the following discussion. The ferroan dolomite and calcite in G.1.1. (Table IV) give $T = 350\,^{\circ}C$ by the method of Bickle and Powell (1977). This involves slight extrapolation of their thermodynamic model, which is untested below 400 °C, but consistent results are obtained from the two limbs of the solvus, suggesting an uncertainty range of approximately $\pm 30\,^{\circ}C$ as discussed by Bickle and Powell (1977). The other assemblages, from approximately the same structural level (fig. 1), presumably represent similar conditions. O.22.5 indicates the problematic nature of the paragonite-muscovite solvus as a geothermometer. The Na/(Na + K) values in paragonite (0.95: Table III) and muscovite (0.16: Evirgen and Ashworth, 1983) both give unrealistically high T estimates from available calibrations (Eugster *et al.*, 1972; Chatterjee and Froese, 1975): in other areas, the two limbs give mutually inconsistent results (e.g. Eugster *et al.*, 1972; Mposkos and Perdikatzis, 1981; Ashworth and Evirgen, 1983). Evidently this solvus is sensitive to minor components and cannot yet provide a useful geothermometer.

Presence of pyrophyllite, rather than kyanite + quartz, places lower limits on a_{H_2O} in the fluid phase in the temperature range $350 \pm 30\,^{\circ}C$ (fig. 5). The

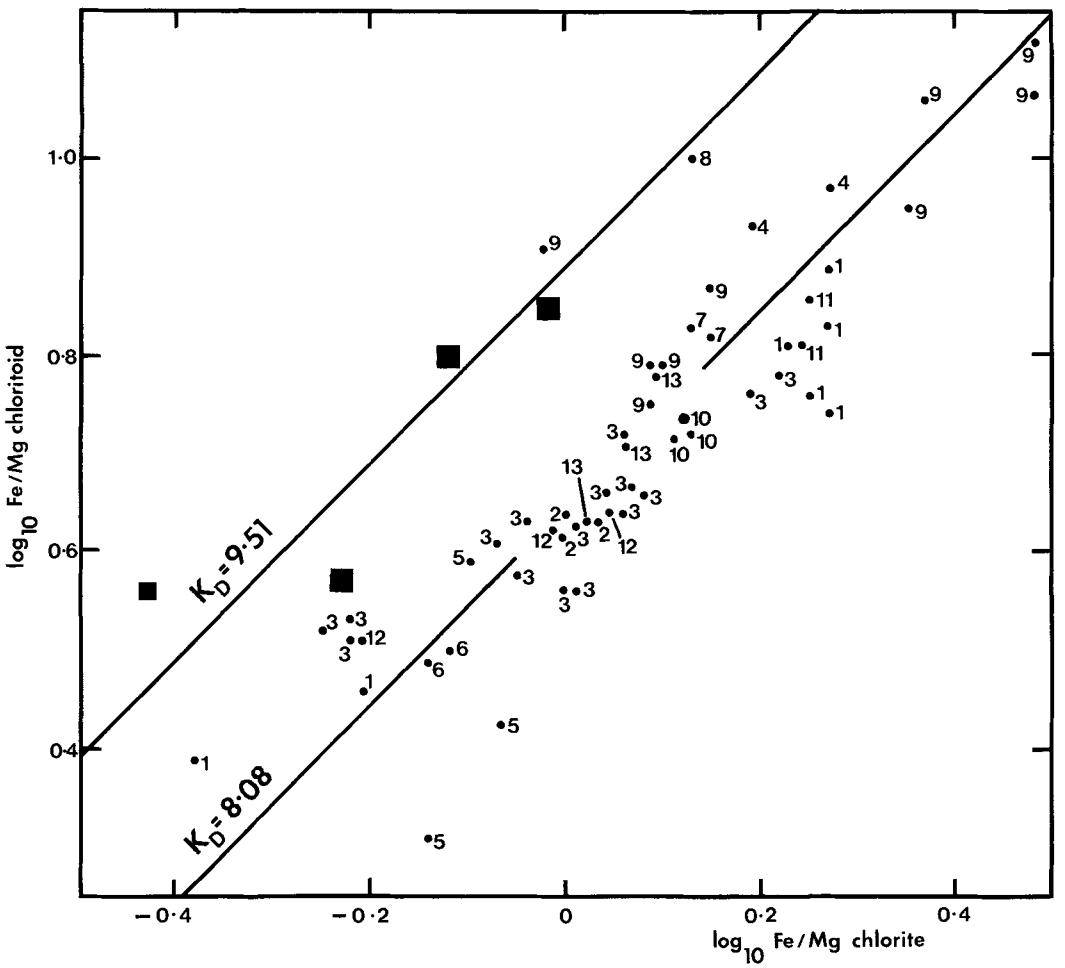

FIG. 4. Fe/Mg partition between chloritoid and chlorite in the study area (solid squares, average logarithmic ratio indicating $K_D = 9.51$) compared with higher-grade areas in the literature (average logarithmic ratio indicating $K_D = 8.08$). Key to literature sources: 1, Albee *et al.* (1965); 2, Fox (1971); 3, Albee (1972); 4, Kramm (1973); 5, Höck (1974); 6, Fox (1975); 7, Cruickshank and Ghent (1978); 8, Liou and Chen (1978); 9, Rumble (1978); 10, Baltatzis (1979); 11, Plimer and Moazez-Lesco (1979); 12, Droop (1981); 13, Ashworth and Evirgen (1983).

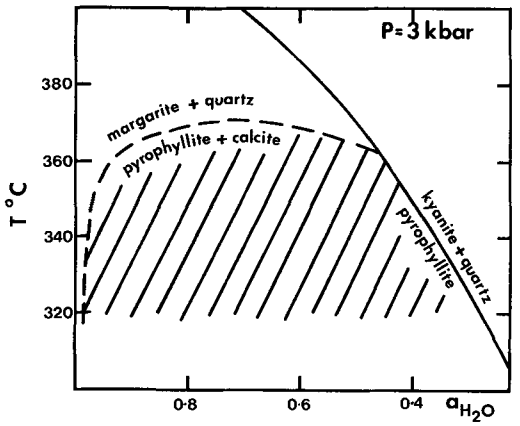

FIG. 5. Likely T-a_{H_2O} conditions of formation of the chloritoid-bearing assemblages with pyprophyllite + calcite (hatched area).

curve is calculated by the method of Powell (1978, p. 246) from thermochemical data of Helgeson *et al.* (1978). Adoption of the data of Haas and Holdaway (1973) would indicate even greater restrictions on a_{H_2O}. The other equilibrium considered in fig. 5, pertinent to the occurrence of pyrophyllite in the carbonate-bearing rocks, is more complicated because it involves CO_2 as well as H_2O:

$$\text{pyrophyllite} + \text{calcite} \rightleftharpoons \text{margarite} + \text{quartz} + H_2O + CO_2.$$

Thus the variation of a_{CO_2} with a_{H_2O} must be considered, at temperatures where mixing is far from ideal. The curve is estimated using the activity-composition diagram of Kerrick and Jacobs (1981, fig. 11) for the lowest temperature they treat (400 °C), and mineral data of Helgeson *et al.* (1978). It shows that coexistence of pyrophyllite with calcite is consistent with high a_{H_2O} in the inferred temperature range.

Thus the pyrophyllite-bearing assembages, with or without calcite, probably formed at $a_{H_2O} \gtrsim 0.4$. Chloritoid is evidently stable at moderate or high a_{H_2O} at temperatures around 350 °C, and these conditions obtained regionally in the metamorphism of the basal Lycian Nappes.

Acknowledgements Electron microprobe facilities were provided by the Department of Metallurgy and Materials Engineering, Aston. We thank the British Council for support, and the MTA Institute (Turkey) and Etibank for logistical assistance in the field. Mr Ö. Ölçer (Aegean Regional Director, MTA Institute) contributed helpful information.

REFERENCES

Albee, A. L. (1972) *Geol. Soc. Am. Bull.* **83,** 3249–68.
——Bingham, E., Chodos, A. A., and Maynes, A. D. (1965) *J. Petrol.* **6,** 246–301.
Ashworth, J. R., and Evirgen, M. M. (1983) *Geol. Mag.* (submitted).
Atherton, M. P. (1980) *J. Earth Sci. R. Dubl. Soc.* **3,** 101–9.
Baltatzis, E. (1979). *Contrib. Mineral. Petrol.* **69,** 193–200.
——(1980) *Neues Jahrb. Mineral. Mh.* 306–13.
Bickle, M. J., and Powell, R. (1977) *Contrib. Mineral. Petrol.* **59,** 281–92.
Brindley, J. C., and Elsdon, R. (1974) *Sci. Proc. R. Soc. Dubl.* **A5,** 123–9.
Çağlayan, M. A., Öztürk, E. M., Öztürk, Z., Sav, H., and Akat, U. (1980) *Jeoloji Mühendisligi*, **10,** 9–17.
Chatterjee, N. D., and Froese, E. (1975) *Am. Mineral.* **60,** 985–93.
Cruickshank, R. D., and Ghent, E. D. (1978) *Contrib. Mineral. Petrol.* **65,** 333–9.
Deer, W. A., Howie, R. A., and Zussman, J. (1982) *Rock-forming Minerals*, Vol. 1A, 2nd edn. Longman, London.
Droop, G. T. R. (1981) *Schweiz. Mineral. Petrogr. Mitt.* **61,** 231–73.
Eugster, H. P., Albee, A. L., Bence, A. E., Thomson, J. B. Jr., and Waldbaum, D. R. (1972) *J. Petrol.* **13,** 147–79.
Evirgen, M. M., and Ashworth, J. R. (1983) *Lithos* (submitted).
Fox, J. S. (1971) *Geol. Mag.* **108,** 205–19.
——(1975) Ibid. **112,** 547–64.
Frey, M. (1978) *J. Petrol.* **19,** 95–135.
Gutnic, M., Monod, O., Poisson, A., and Dumont, J. (1979) *Mem. Soc. Geol. Fr.* **137.**
Haas, H., and Holdaway, M. J. (1973) *Am. J. Sci.* **273,** 449–64.
Hålenius, U., Annersten, H., and Langer K. (1981) *Phys. Chem. Minerals* **7,** 117–23.
Helgeson, H. C., Delany, J. M., Nesbitt, H. W., and Bird, D. K. (1978) *Am. J. Sci.* **278-A.**
Höck, V. (1974) *Schweiz. Mineral. Petrogr. Mitt.* **54,** 567–93.
Hollister, L. S. (1969) *Geol. Soc. Am. Bull.* **80,** 2465–94.
Hoschek, G. (1969) *Contib. Mineral. Petrol.* **22,** 208–32.
Katagas, C., and Sapountzis, E. (977) *Neues Jahrb Miner. Abh.* **129,** 100–12.
Kerrick, D. M., and Jacobs, G. K. (1981) *Am. J. Sci.* **281,** 735–67.
Kramm, U. (1973) *Contrib. Mineral. Petrol.* **41,** 179–96.
Liou, J. G., and Chen, P.-Y. (1978) *Lithos*, **11,** 175–87.
Mposkos, E., and Perdikatzis, V. (1981) *Neues Jahrb. Miner. Abh.* **142,** 292–308.
Plimer, I. R., and Moazez-Lesco, Z. (1979) Ibid. **135,** 180–9.
Powell, R. (1978) *Equilibrium Thermodynamics in Petrology.* Harper and Row, London.
Rumble, D. III (1978) *J. Petrol.* **19,** 317–40.
Thompson, A. B. (1976) *Am. J. Sci.* **276,** 401–54.
Thompson, J. B. Jr., and Norton, S. A. (1968) In *Studies in Appalachian Geology, Northern and Maritime* (Zen, E-an *et al.*, eds.). Interscience, New York 319–27.
Winkler, H. G. F. (1979) *Petrogenesis of Metamorphic Rocks*, 5th edn. Springer-Verlag, New York.
Zen, E-an (1960) *Am. Mineral.* **45,** 129–75.

[*Manuscript received 8 August 1983; revised 2 November 1983*]